

Determination of the number of $\psi(3686)$ events taken at BESIII *

M. Ablikim¹, M. N. Achasov^{4,c}, P. Adlarson⁷⁵, O. Afedulidis³, X. C. Ai⁸⁰, R. Aliberti³⁵, A. Amoroso^{74A,74C}, Q. An^{71,58,a}, Y. Bai⁵⁷, O. Bakina³⁶, I. Balossino^{29A}, Y. Ban^{46,h}, H.-R. Bao⁶³, V. Batzskaya^{1,44}, K. Begzsuren³², N. Berger³⁵, M. Berlowski⁴⁴, M. Bertani^{28A}, D. Bettoni^{29A}, F. Bianchi^{74A,74C}, E. Bianco^{74A,74C}, A. Bortone^{74A,74C}, I. Boyko³⁶, R. A. Briere⁵, A. Brueggemann⁶⁸, H. Cai⁷⁶, X. Cai^{1,58}, A. Calcaterra^{28A}, G. F. Cao^{1,63}, N. Cao^{1,63}, S. A. Cetin^{62A}, J. F. Chang^{1,58}, G. R. Che⁴³, G. Chelkov^{36,b}, C. Chen⁴³, C. H. Chen⁹, Chao Chen⁵⁵, G. Chen¹, H. S. Chen^{1,63}, H. Y. Chen²⁰, M. L. Chen^{1,58,63}, S. J. Chen⁴², S. L. Chen⁴⁵, S. M. Chen⁶¹, T. Chen^{1,63}, X. R. Chen^{31,63}, X. T. Chen^{1,63}, Y. B. Chen^{1,58}, Y. Q. Chen³⁴, Z. J. Chen^{25,i}, Z. Y. Chen^{1,63}, S. K. Choi^{10A}, G. Cibinetto^{29A}, F. Cossio^{74C}, J. J. Cui⁵⁰, H. L. Dai^{1,58}, J. P. Dai⁷⁸, A. Dbeyssi¹⁸, R. E. de Boer³, D. Dedovich³⁶, C. Q. Deng⁷², Z. Y. Deng¹, A. Denig³⁵, I. Denysenko³⁶, M. Destefanis^{74A,74C}, F. De Mori^{74A,74C}, B. Ding^{66,1}, X. X. Ding^{46,h}, Y. Ding⁴⁰, Y. Ding³⁴, J. Dong^{1,58}, L. Y. Dong^{1,63}, M. Y. Dong^{1,58,63}, X. Dong⁷⁶, M. C. Du¹, S. X. Du⁸⁰, Y. Y. Duan⁵⁵, Z. H. Duan⁴², P. Egorov^{36,b}, Y. H. Fan⁴⁵, J. Fang^{1,58}, J. Fang⁵⁹, S. S. Fang^{1,63}, W. X. Fang¹, Y. Fang¹, Y. Q. Fang^{1,58}, R. Farinelli^{29A}, L. Fava^{74B,74C}, F. Feldbauer³, G. Felici^{28A}, C. Q. Feng^{71,58}, J. H. Feng⁵⁹, Y. T. Feng^{71,58}, M. Fritsch³, C. D. Fu¹, J. L. Fu⁶³, Y. W. Fu^{1,63}, H. Gao⁶³, X. B. Gao⁴¹, Y. N. Gao^{46,h}, Yang Gao^{71,58}, S. Garbolino^{74C}, I. Garzia^{29A,29B}, L. Ge⁸⁰, P. T. Ge⁷⁶, Z. W. Ge⁴², C. Geng⁵⁹, E. M. Gersabeck⁶⁷, A. Gilman⁶⁹, K. Goetzen¹³, L. Gong⁴⁰, W. X. Gong^{1,58}, W. Gradl³⁵, S. Gramigna^{29A,29B}, M. Greco^{74A,74C}, M. H. Gu^{1,58}, Y. T. Gu¹⁵, C. Y. Guan^{1,63}, Z. L. Guan²², A. Q. Guo^{31,63}, L. B. Guo⁴¹, M. J. Guo⁵⁰, R. P. Guo⁴⁹, Y. P. Guo^{12,g}, A. Guskov^{36,b}, J. Gutierrez²⁷, K. L. Han⁶³, T. T. Han¹, F. Hanisch³, X. Q. Hao¹⁹, F. A. Harris⁶⁵, K. K. He⁵⁵, K. L. He^{1,63}, F. H. Heinsius³, C. H. Heinz³⁵, Y. K. Heng^{1,58,63}, C. Herold⁶⁰, T. Holtmann³, P. C. Hong³⁴, G. Y. Hou^{1,63}, X. T. Hou^{1,63}, Y. R. Hou⁶³, Z. L. Hou¹, B. Y. Hu⁵⁹, H. M. Hu^{1,63}, J. F. Hu^{56,j}, S. L. Hu^{12,g}, T. Hu^{1,58,63}, Y. Hu¹, G. S. Huang^{71,58}, K. X. Huang⁵⁹, L. Q. Huang^{31,63}, X. T. Huang⁵⁰, Y. P. Huang¹, T. Hussain⁷³, F. Hölzken³, N. Hüsken³⁵, N. Hüsken^{27,35}, N. in der Wiesche⁶⁸, J. Jackson²⁷, S. Janchiv³², J. H. Jeong^{10A}, Q. Ji¹, Q. P. Ji¹⁹, W. Ji^{1,63}, X. B. Ji^{1,63}, X. L. Ji^{1,58}, Y. Y. Ji⁵⁰, X. Q. Jia⁵⁰, Z. K. Jia^{71,58}, D. Jiang^{1,63}, H. B. Jiang⁷⁶, P. C. Jiang^{46,h}, S. S. Jiang³⁹, T. J. Jiang¹⁶, X. S. Jiang^{1,58,63}, Y. Jiang⁶³, J. B. Jiao⁵⁰, J. K. Jiao³⁴, Z. Jiao²³, S. Jin⁴², Y. Jin⁶⁶, M. Q. Jing^{1,63}, X. M. Jing⁶³, T. Johansson⁷⁵, S. Kabana³³, N. Kalantar-Nayestanaki⁶⁴, X. L. Kang⁹, X. S. Kang⁴⁰, M. Kavatsyuk⁶⁴, B. C. Ke⁸⁰, V. Khachatryan²⁷, A. Khoukaz⁶⁸, R. Kiuchi¹, O. B. Kolcu^{62A}, B. Kopf³, M. Kuessner³, X. Kui^{1,63}, N. Kumar²⁶, A. Kupsc^{44,75}, W. Kühn³⁷, J. J. Lane⁶⁷, P. Larin¹⁸, L. Lavezzi^{74A,74C}, T. T. Lei^{71,58}, Z. H. Lei^{71,58}, M. Lellmann³⁵, T. Lenz³⁵, C. Li⁴³, C. Li⁴⁷, C. H. Li³⁹, Cheng Li^{71,58}, D. M. Li⁸⁰, F. Li^{1,58}, G. Li¹, H. B. Li^{1,63}, H. J. Li¹⁹, H. N. Li^{56,j}, Hui Li⁴³, J. R. Li⁶¹, J. S. Li⁵⁹, Ke Li¹, L. J. Li^{1,63}, L. K. Li¹, Lei Li⁴⁸, M. H. Li⁴³, P. R. Li^{38,k,l}, Q. M. Li^{1,63}, Q. X. Li⁵⁰, R. Li^{17,31}, S. X. Li¹², T. Li⁵⁰,

Received xxxx December xxxx

* The BESIII Collaboration thanks the staff of BEPCII and the IHEP computing center for their strong support. This work is supported in part by National Key R&D Program of China under Contracts Nos. 2020YFA0406300, 2020YFA0406400; National Natural Science Foundation of China (NSFC) under Contracts Nos. 12150004, 11635010, 11735014, 11835012, 11935015, 11935016, 11935018, 11961141012, 12025502, 12035009, 12035013, 12061131003, 12192260, 12192261, 12192262, 12192263, 12192264, 12192265, 12221005, 12225509, 12235017; the Program of Science and Technology Development Plan of Jilin Province of China under Contract No. 20210508047RQ and 20230101021JC; the Chinese Academy of Sciences (CAS) Large-Scale Scientific Facility Program; the CAS Center for Excellence in Particle Physics (CCEPP); Joint Large-Scale Scientific Facility Funds of the NSFC and CAS under Contract No. U1832207; CAS Key Research Program of Frontier Sciences under Contracts Nos. QYZDJ-SSW-SLH003, QYZDJ-SSW-SLH040; 100 Talents Program of CAS; The Institute of Nuclear and Particle Physics (INPAC) and Shanghai Key Laboratory for Particle Physics and Cosmology; European Union's Horizon 2020 research and innovation programme under Marie Skłodowska-Curie grant agreement under Contract No. 894790; German Research Foundation DFG under Contracts Nos. 455635585, Collaborative Research Center CRC 1044, FOR5327, GRK 2149; Istituto Nazionale di Fisica Nucleare, Italy; Ministry of Development of Turkey under Contract No. DPT2006K-120470; National Research Foundation of Korea under Contract No. NRF-2022R1A2C1092335; National Science and Technology fund of Mongolia; National Science Research and Innovation Fund (NSRF) via the Program Management Unit for Human Resources & Institutional Development, Research and Innovation of Thailand under Contract No. B16F640076; Polish National Science Centre under Contract No. 2019/35/O/ST2/02907; The Swedish Research Council; U. S. Department of Energy under Contract No. DE-FG02-05ER41374.

W. D. Li^{1,63}, W. G. Li^{1,a}, X. Li^{1,63}, X. H. Li^{71,58}, X. L. Li⁵⁰, X. Z. Li⁵⁹, Xiaoyu Li^{1,63}, Y. G. Li^{46,h}, Z. J. Li⁵⁹, Z. X. Li¹⁵, Z. Y. Li⁷⁸, C. Liang⁴², H. Liang^{1,63}, H. Liang^{71,58}, Y. F. Liang⁵⁴, Y. T. Liang^{31,63}, G. R. Liao¹⁴, L. Z. Liao⁵⁰, J. Libby²⁶, A. Limphirat⁶⁰, C. C. Lin⁵⁵, D. X. Lin^{31,63}, T. Lin¹, B. J. Liu¹, B. X. Liu⁷⁶, C. Liu³⁴, C. X. Liu¹, F. H. Liu⁵³, Fang Liu¹, Feng Liu⁶, G. M. Liu^{56,j}, H. Liu^{38,k,l}, H. B. Liu¹⁵, H. M. Liu^{1,63}, Huanhuan Liu¹, Huihui Liu²¹, J. B. Liu^{71,58}, J. Y. Liu^{1,63}, K. Liu^{38,k,l}, K. Y. Liu⁴⁰, Ke Liu²², L. Liu^{71,58}, L. C. Liu⁴³, Lu Liu⁴³, M. H. Liu^{12,g}, P. L. Liu¹, Q. Liu⁶³, S. B. Liu^{71,58}, T. Liu^{12,g}, W. K. Liu⁴³, W. M. Liu^{71,58}, X. Liu^{38,k,l}, X. Liu³⁹, Y. Liu^{38,k,l}, Y. Liu⁸⁰, Y. B. Liu⁴³, Z. A. Liu^{1,58,63}, Z. D. Liu⁹, Z. Q. Liu⁵⁰, X. C. Lou^{1,58,63}, F. X. Lu⁵⁹, H. J. Lu²³, J. G. Lu^{1,58}, X. L. Lu¹, Y. Lu⁷, Y. P. Lu^{1,58}, Z. H. Lu^{1,63}, C. L. Luo⁴¹, J. R. Luo⁵⁹, M. X. Luo⁷⁹, T. Luo^{12,g}, X. L. Luo^{1,58}, X. R. Lyu⁶³, Y. F. Lyu⁴³, F. C. Ma⁴⁰, H. Ma⁷⁸, H. L. Ma¹, J. L. Ma^{1,63}, L. L. Ma⁵⁰, M. M. Ma^{1,63}, Q. M. Ma¹, R. Q. Ma^{1,63}, T. Ma^{71,58}, X. T. Ma^{1,63}, X. Y. Ma^{1,58}, Y. Ma^{46,h}, Y. M. Ma³¹, F. E. Maas¹⁸, M. Maggiora^{74A,74C}, S. Malde⁶⁹, Y. J. Mao^{46,h}, Z. P. Mao¹, S. Marcello^{74A,74C}, Z. X. Meng⁶⁶, J. G. Messchendorp^{13,64}, G. Mezzadri^{29A}, H. Miao^{1,63}, T. J. Min⁴², R. E. Mitchell²⁷, X. H. Mo^{1,58,63}, B. Moses²⁷, N. Yu. Muchnoi^{4,c}, J. Muskalla³⁵, Y. Nefedov³⁶, F. Nerling^{18,e}, L. S. Nie²⁰, I. B. Nikolaev^{4,c}, Z. Ning^{1,58}, S. Nisar^{11,m}, Q. L. Niu^{38,k,l}, W. D. Niu⁵⁵, Y. Niu⁵⁰, S. L. Olsen⁶³, Q. Ouyang^{1,58,63}, S. Pacetti^{28B,28C}, X. Pan⁵⁵, Y. Pan⁵⁷, A. Pathak³⁴, P. Patteri^{28A}, Y. P. Pei^{71,58}, M. Pelizaeus³, H. P. Peng^{71,58}, Y. Y. Peng^{38,k,l}, K. Peters^{13,e}, J. L. Ping⁴¹, R. G. Ping^{1,63}, S. Plura³⁵, V. Prasad³³, F. Z. Qi¹, H. Qi^{71,58}, H. R. Qi⁶¹, M. Qi⁴², T. Y. Qi^{12,g}, S. Qian^{1,58}, W. B. Qian⁶³, C. F. Qiao⁶³, X. K. Qiao⁸⁰, J. J. Qin⁷², L. Q. Qin¹⁴, L. Y. Qin^{71,58}, X. S. Qin⁵⁰, Z. H. Qin^{1,58}, J. F. Qiu¹, Z. H. Qu⁷², C. F. Redmer³⁵, K. J. Ren³⁹, A. Rivetti^{74C}, M. Rolo^{74C}, G. Rong^{1,63}, Ch. Rosner¹⁸, S. N. Ruan⁴³, N. Salone⁴⁴, A. Sarantsev^{36,d}, Y. Schelhaas³⁵, K. Schoenning⁷⁵, M. Scodeggio^{29A}, K. Y. Shan^{12,g}, W. Shan²⁴, X. Y. Shan^{71,58}, Z. J. Shang^{38,k,l}, J. F. Shangguan⁵⁵, L. G. Shao^{1,63}, M. Shao^{71,58}, C. P. Shen^{12,g}, H. F. Shen^{1,8}, W. H. Shen⁶³, X. Y. Shen^{1,63}, B. A. Shi⁶³, H. Shi^{71,58}, H. C. Shi^{71,58}, J. L. Shi^{12,g}, J. Y. Shi¹, Q. Q. Shi⁵⁵, S. Y. Shi⁷², X. Shi^{1,58}, J. J. Song¹⁹, T. Z. Song⁵⁹, W. M. Song^{34,1}, Y. J. Song^{12,g}, Y. X. Song^{46,h,n}, S. Sosio^{74A,74C}, S. Spataro^{74A,74C}, F. Stieler³⁵, Y. J. Su⁶³, G. B. Sun⁷⁶, G. X. Sun¹, H. Sun⁶³, H. K. Sun¹, J. F. Sun¹⁹, K. Sun⁶¹, L. Sun⁷⁶, S. S. Sun^{1,63}, T. Sun^{51,f}, W. Y. Sun³⁴, Y. Sun⁹, Y. J. Sun^{71,58}, Y. Z. Sun¹, Z. Q. Sun^{1,63}, Z. T. Sun⁵⁰, C. J. Tang⁵⁴, G. Y. Tang¹, J. Tang⁵⁹, M. Tang^{71,58}, Y. A. Tang⁷⁶, L. Y. Tao⁷², Q. T. Tao^{25,i}, M. Tat⁶⁹, J. X. Teng^{71,58}, V. Thoren⁷⁵, W. H. Tian⁵⁹, Y. Tian^{31,63}, Z. F. Tian⁷⁶, I. Uman^{62B}, Y. Wan⁵⁵, S. J. Wang⁵⁰, B. Wang¹, B. L. Wang⁶³, Bo Wang^{71,58}, D. Y. Wang^{46,h}, F. Wang⁷², H. J. Wang^{38,k,l}, J. J. Wang⁷⁶, J. P. Wang⁵⁰, K. Wang^{1,58}, L. L. Wang¹, M. Wang⁵⁰, N. Y. Wang⁶³, S. Wang^{12,g}, S. Wang^{38,k,l}, T. Wang^{12,g}, T. J. Wang⁴³, W. Wang⁷², W. Wang⁵⁹, W. P. Wang^{35,71,o}, X. Wang^{46,h}, X. F. Wang^{38,k,l}, X. J. Wang³⁹, X. L. Wang^{12,g}, X. N. Wang¹, Y. Wang⁶¹, Y. D. Wang⁴⁵, Y. F. Wang^{1,58,63}, Y. L. Wang¹⁹, Y. N. Wang⁴⁵, Y. Q. Wang¹, Yaqian Wang¹⁷, Yi Wang⁶¹, Z. Wang^{1,58}, Z. L. Wang⁷², Z. Y. Wang^{1,63}, Ziyi Wang⁶³, D. H. Wei¹⁴, F. Weidner⁶⁸, S. P. Wen¹, Y. R. Wen³⁹, U. Wiedner³, G. Wilkinson⁶⁹, M. Wolke⁷⁵, L. Wollenberg³, C. Wu³⁹, J. F. Wu^{1,8}, L. H. Wu¹, L. J. Wu^{1,63}, X. Wu^{12,g}, X. H. Wu³⁴, Y. Wu^{71,58}, Y. H. Wu⁵⁵, Y. J. Wu³¹, Z. Wu^{1,58}, L. Xia^{71,58}, X. M. Xian³⁹, B. H. Xiang^{1,63}, T. Xiang^{46,h}, D. Xiao^{38,k,l}, G. Y. Xiao⁴², S. Y. Xiao¹, Y. L. Xiao^{12,g}, Z. J. Xiao⁴¹, C. Xie⁴², X. H. Xie^{46,h}, Y. Xie⁵⁰, Y. G. Xie^{1,58}, Y. H. Xie⁶, Z. P. Xie^{71,58}, T. Y. Xing^{1,63}, C. F. Xu^{1,63}, C. J. Xu⁵⁹, G. F. Xu¹, H. Y. Xu^{66,2,p}, M. Xu^{71,58}, Q. J. Xu¹⁶, Q. N. Xu³⁰, W. Xu¹, W. L. Xu⁶⁶, X. P. Xu⁵⁵, Y. C. Xu⁷⁷, Z. P. Xu⁴², Z. S. Xu⁶³, F. Yan^{12,g}, L. Yan^{12,g}, W. B. Yan^{71,58}, W. C. Yan⁸⁰, X. Q. Yan¹, H. J. Yang^{51,f}, H. L. Yang³⁴, H. X. Yang¹, Tao Yang¹, Y. Yang^{12,g}, Y. F. Yang⁴³, Y. X. Yang^{1,63}, Yifan Yang^{1,63}, Z. W. Yang^{38,k,l}, Z. P. Yao⁵⁰, M. Ye^{1,58}, M. H. Ye⁸, J. H. Yin¹, Z. Y. You⁵⁹, B. X. Yu^{1,58,63}, C. X. Yu⁴³, G. Yu^{1,63}, J. S. Yu^{25,i}, T. Yu⁷², X. D. Yu^{46,h}, Y. C. Yu⁸⁰, C. Z. Yuan^{1,63}, J. Yuan⁴⁵, J. Yuan³⁴, L. Yuan², S. C. Yuan¹, Y. Yuan^{1,63}, Z. Y. Yuan⁵⁹, C. X. Yue³⁹, A. A. Zafar⁷³, F. R. Zeng⁵⁰, S. H. Zeng⁷², X. Zeng^{12,g}, Y. Zeng^{25,i}, Y. J. Zeng⁵⁹, Y. J. Zeng^{1,63}, X. Y. Zhai³⁴, Y. C. Zhai⁵⁰, Y. H. Zhan⁵⁹, A. Q. Zhang^{1,63}, B. L. Zhang^{1,63}, B. X. Zhang¹, D. H. Zhang⁴³, G. Y. Zhang¹⁹, H. Zhang^{71,58}, H. Zhang⁸⁰, H. C. Zhang^{1,58,63}, H. H. Zhang³⁴, H. H. Zhang⁵⁹, H. Q. Zhang^{1,58,63}, H. R. Zhang^{71,58}, H. Y. Zhang^{1,58}, J. Zhang⁵⁹, J. Zhang⁸⁰, J. J. Zhang⁵², J. L. Zhang²⁰, J. Q. Zhang⁴¹, J. S. Zhang^{12,g}, J. W. Zhang^{1,58,63}, J. X. Zhang^{38,k,l}, J. Y. Zhang¹, J. Z. Zhang^{1,63}, Jianyu Zhang⁶³, L. M. Zhang⁶¹, Lei Zhang⁴², P. Zhang^{1,63}, Q. Y. Zhang³⁴, R. Y. Zhang^{38,k,l}, Shuihan Zhang^{1,63}, Shulei Zhang^{25,i}, X. D. Zhang⁴⁵, X. M. Zhang¹, X. Y. Zhang⁵⁰, Y. Zhang⁷², Y. T. Zhang⁸⁰, Y. H. Zhang^{1,58}, Y. M. Zhang³⁹, Yan Zhang^{71,58}, Yao Zhang¹, Z. D. Zhang¹, Z. H. Zhang¹, Z. L. Zhang³⁴, Z. Y. Zhang⁷⁶, Z. Y. Zhang⁴³, Z. Z. Zhang⁴⁵, G. Zhao¹, J. Y. Zhao^{1,63}, J. Z. Zhao^{1,58}, Lei Zhao^{71,58}, Ling Zhao¹, M. G. Zhao⁴³, N. Zhao⁷⁸, R. P. Zhao⁶³, S. J. Zhao⁸⁰, Y. B. Zhao^{1,58},

Y. X. Zhao^{31,63}, Z. G. Zhao^{71,58}, A. Zhemchugov^{36,b}, B. Zheng⁷², B. M. Zheng³⁴, J. P. Zheng^{1,58},
W. J. Zheng^{1,63}, Y. H. Zheng⁶³, B. Zhong⁴¹, X. Zhong⁵⁹, H. Zhou⁵⁰, J. Y. Zhou³⁴, L. P. Zhou^{1,63}, S. Zhou⁶,
X. Zhou⁷⁶, X. K. Zhou⁶, X. R. Zhou^{71,58}, X. Y. Zhou³⁹, Y. Z. Zhou^{12,g}, J. Zhu⁴³, K. Zhu¹, K. J. Zhu^{1,58,63},
K. S. Zhu^{12,g}, L. Zhu³⁴, L. X. Zhu⁶³, S. H. Zhu⁷⁰, S. Q. Zhu⁴², T. J. Zhu^{12,g}, W. D. Zhu⁴¹, Y. C. Zhu^{71,58},
Z. A. Zhu^{1,63}, J. H. Zou¹, J. Zu^{71,58}

(BESIII Collaboration)

¹ Institute of High Energy Physics, Beijing 100049, People's Republic of China

² Beihang University, Beijing 100191, People's Republic of China

³ Bochum Ruhr-University, D-44780 Bochum, Germany

⁴ Budker Institute of Nuclear Physics SB RAS (BINP), Novosibirsk 630090, Russia

⁵ Carnegie Mellon University, Pittsburgh, Pennsylvania 15213, USA

⁶ Central China Normal University, Wuhan 430079, People's Republic of China

⁷ Central South University, Changsha 410083, People's Republic of China

⁸ China Center of Advanced Science and Technology, Beijing 100190, People's Republic of China

⁹ China University of Geosciences, Wuhan 430074, People's Republic of China

¹⁰ Chung-Ang University, Seoul, 06974, Republic of Korea

¹¹ COMSATS University Islamabad, Lahore Campus, Defence Road, Off Raiwind Road, 54000 Lahore, Pakistan

¹² Fudan University, Shanghai 200433, People's Republic of China

¹³ GSI Helmholtzcentre for Heavy Ion Research GmbH, D-64291 Darmstadt, Germany

¹⁴ Guangxi Normal University, Guilin 541004, People's Republic of China

¹⁵ Guangxi University, Nanning 530004, People's Republic of China

¹⁶ Hangzhou Normal University, Hangzhou 310036, People's Republic of China

¹⁷ Hebei University, Baoding 071002, People's Republic of China

¹⁸ Helmholtz Institute Mainz, Staudinger Weg 18, D-55099 Mainz, Germany

¹⁹ Henan Normal University, Xinxiang 453007, People's Republic of China

²⁰ Henan University, Kaifeng 475004, People's Republic of China

²¹ Henan University of Science and Technology, Luoyang 471003, People's Republic of China

²² Henan University of Technology, Zhengzhou 450001, People's Republic of China

²³ Huangshan College, Huangshan 245000, People's Republic of China

²⁴ Hunan Normal University, Changsha 410081, People's Republic of China

²⁵ Hunan University, Changsha 410082, People's Republic of China

²⁶ Indian Institute of Technology Madras, Chennai 600036, India

²⁷ Indiana University, Bloomington, Indiana 47405, USA

²⁸ INFN Laboratori Nazionali di Frascati, (A)INFN Laboratori Nazionali di Frascati, I-00044, Frascati, Italy;
(B)INFN Sezione di Perugia, I-06100, Perugia, Italy; (C)University of Perugia, I-06100, Perugia, Italy

²⁹ INFN Sezione di Ferrara, (A)INFN Sezione di Ferrara, I-44122, Ferrara, Italy; (B)University of Ferrara,
I-44122, Ferrara, Italy

³⁰ Inner Mongolia University, Hohhot 010021, People's Republic of China

³¹ Institute of Modern Physics, Lanzhou 730000, People's Republic of China

³² Institute of Physics and Technology, Peace Avenue 54B, Ulaanbaatar 13330, Mongolia

³³ Instituto de Alta Investigación, Universidad de Tarapacá, Casilla 7D, Arica 1000000, Chile

³⁴ Jilin University, Changchun 130012, People's Republic of China

³⁵ Johannes Gutenberg University of Mainz, Johann-Joachim-Becher-Weg 45, D-55099 Mainz, Germany

³⁶ Joint Institute for Nuclear Research, 141980 Dubna, Moscow region, Russia

³⁷ Justus-Liebig-Universität Giessen, II. Physikalisches Institut, Heinrich-Buff-Ring 16, D-35392 Giessen,
Germany

³⁸ Lanzhou University, Lanzhou 730000, People's Republic of China

³⁹ Liaoning Normal University, Dalian 116029, People's Republic of China

⁴⁰ Liaoning University, Shenyang 110036, People's Republic of China

⁴¹ Nanjing Normal University, Nanjing 210023, People's Republic of China

- ⁴² Nanjing University, Nanjing 210093, People's Republic of China
- ⁴³ Nankai University, Tianjin 300071, People's Republic of China
- ⁴⁴ National Centre for Nuclear Research, Warsaw 02-093, Poland
- ⁴⁵ North China Electric Power University, Beijing 102206, People's Republic of China
- ⁴⁶ Peking University, Beijing 100871, People's Republic of China
- ⁴⁷ Qufu Normal University, Qufu 273165, People's Republic of China
- ⁴⁸ Renmin University of China, Beijing 100872, People's Republic of China
- ⁴⁹ Shandong Normal University, Jinan 250014, People's Republic of China
- ⁵⁰ Shandong University, Jinan 250100, People's Republic of China
- ⁵¹ Shanghai Jiao Tong University, Shanghai 200240, People's Republic of China
- ⁵² Shanxi Normal University, Linfen 041004, People's Republic of China
- ⁵³ Shanxi University, Taiyuan 030006, People's Republic of China
- ⁵⁴ Sichuan University, Chengdu 610064, People's Republic of China
- ⁵⁵ Soochow University, Suzhou 215006, People's Republic of China
- ⁵⁶ South China Normal University, Guangzhou 510006, People's Republic of China
- ⁵⁷ Southeast University, Nanjing 211100, People's Republic of China
- ⁵⁸ State Key Laboratory of Particle Detection and Electronics, Beijing 100049, Hefei 230026, People's Republic of China
- ⁵⁹ Sun Yat-Sen University, Guangzhou 510275, People's Republic of China
- ⁶⁰ Suranaree University of Technology, University Avenue 111, Nakhon Ratchasima 30000, Thailand
- ⁶¹ Tsinghua University, Beijing 100084, People's Republic of China
- ⁶² Turkish Accelerator Center Particle Factory Group, (A)Istinye University, 34010, Istanbul, Turkey; (B)Near East University, Nicosia, North Cyprus, 99138, Mersin 10, Turkey
- ⁶³ University of Chinese Academy of Sciences, Beijing 100049, People's Republic of China
- ⁶⁴ University of Groningen, NL-9747 AA Groningen, The Netherlands
- ⁶⁵ University of Hawaii, Honolulu, Hawaii 96822, USA
- ⁶⁶ University of Jinan, Jinan 250022, People's Republic of China
- ⁶⁷ University of Manchester, Oxford Road, Manchester, M13 9PL, United Kingdom
- ⁶⁸ University of Muenster, Wilhelm-Klemm-Strasse 9, 48149 Muenster, Germany
- ⁶⁹ University of Oxford, Keble Road, Oxford OX13RH, United Kingdom
- ⁷⁰ University of Science and Technology Liaoning, Anshan 114051, People's Republic of China
- ⁷¹ University of Science and Technology of China, Hefei 230026, People's Republic of China
- ⁷² University of South China, Hengyang 421001, People's Republic of China
- ⁷³ University of the Punjab, Lahore-54590, Pakistan
- ⁷⁴ University of Turin and INFN, (A)University of Turin, I-10125, Turin, Italy; (B)University of Eastern Piedmont, I-15121, Alessandria, Italy; (C)INFN, I-10125, Turin, Italy
- ⁷⁵ Uppsala University, Box 516, SE-75120 Uppsala, Sweden
- ⁷⁶ Wuhan University, Wuhan 430072, People's Republic of China
- ⁷⁷ Yantai University, Yantai 264005, People's Republic of China
- ⁷⁸ Yunnan University, Kunming 650500, People's Republic of China
- ⁷⁹ Zhejiang University, Hangzhou 310027, People's Republic of China
- ⁸⁰ Zhengzhou University, Zhengzhou 450001, People's Republic of China
- ^a Deceased
- ^b Also at the Moscow Institute of Physics and Technology, Moscow 141700, Russia
- ^c Also at the Novosibirsk State University, Novosibirsk, 630090, Russia
- ^d Also at the NRC "Kurchatov Institute", PNPI, 188300, Gatchina, Russia
- ^e Also at Goethe University Frankfurt, 60323 Frankfurt am Main, Germany
- ^f Also at Key Laboratory for Particle Physics, Astrophysics and Cosmology, Ministry of Education; Shanghai Key Laboratory for Particle Physics and Cosmology; Institute of Nuclear and Particle Physics, Shanghai 200240, People's Republic of China
- ^g Also at Key Laboratory of Nuclear Physics and Ion-beam Application (MOE) and Institute of Modern

Physics, Fudan University, Shanghai 200443, People's Republic of China

^h *Also at State Key Laboratory of Nuclear Physics and Technology, Peking University, Beijing 100871, People's Republic of China*

ⁱ *Also at School of Physics and Electronics, Hunan University, Changsha 410082, China*

^j *Also at Guangdong Provincial Key Laboratory of Nuclear Science, Institute of Quantum Matter, South China Normal University, Guangzhou 510006, China*

^k *Also at MOE Frontiers Science Center for Rare Isotopes, Lanzhou University, Lanzhou 730000, People's Republic of China*

^l *Also at Lanzhou Center for Theoretical Physics, Lanzhou University, Lanzhou 730000, People's Republic of China*

^m *Also at the Department of Mathematical Sciences, IBA, Karachi 75270, Pakistan*

ⁿ *Also at Ecole Polytechnique Federale de Lausanne (EPFL), CH-1015 Lausanne, Switzerland*

^o *Also at Helmholtz Institute Mainz, Staudinger Weg 18, D-55099 Mainz, Germany*

^p *Also at School of Physics, Beihang University, Beijing 100191, China*

Abstract The number of $\psi(3686)$ events collected by the BESIII detector during the 2021 run period is determined to be $(2259.3 \pm 11.1) \times 10^6$ by counting inclusive $\psi(3686)$ hadronic events. The uncertainty is systematic and the statistical uncertainty is negligible. Meanwhile, the numbers of $\psi(3686)$ events collected during the 2009 and 2012 run periods are updated to be $(107.7 \pm 0.6) \times 10^6$ and $(345.4 \pm 2.6) \times 10^6$, respectively. Both numbers are consistent with the previous measurements within one standard deviation. The total number of $\psi(3686)$ events in the three data samples is $(2712.4 \pm 14.3) \times 10^6$.

Key words $\psi(3686)$, inclusive process, hadronic events, BESIII detector

1 Introduction

In 2009, 2012, and 2021, the BESIII experiment accumulated the world's largest $\psi(3686)$ data sample produced in electron-positron collisions, thereby providing an excellent platform to precisely study the transitions and decays of the $\psi(3686)$ and its daughter charmonium states, including the χ_{cJ} , h_c , and η_c , and to search for rare decays with physics beyond the Standard Model. The number of $\psi(3686)$ events, $N_{\psi(3686)}$, is a basic input parameter, and its precision has a direct impact on the accuracy of these measurements.

In this paper, we determine the number of $\psi(3686)$ events by using inclusive $\psi(3686)$ hadronic decays, where the branching fraction of $\psi(3686) \rightarrow \text{hadrons}$ is known to be $(97.85 \pm 0.13)\%$ [1–3]. The nonresonant background yield under the $\psi(3686)$ peak is evaluated by analyzing the two off-resonance data samples taken in 2009 and 2021 at center-of-mass (c.m.) energy $E_{\text{cm}} = 3.65$ GeV. The same method of background estimation was successfully used in our previous measurement of the numbers of $\psi(3686)$ events in the data samples collected in 2009 and 2012 [4].

2 BEPCII and BESIII Detector

BEPCII [5] is a double-ring e^+e^- collider in the center-of-mass energy range from 2.0 to 4.95 GeV

which has reached a peak luminosity of $1 \times 10^{33} \text{ cm}^{-2} \text{ s}^{-1}$ at $\sqrt{s} = 3.773$ GeV. The cylindrical core of the BESIII detector [5] consists of a helium-based multilayer drift chamber (MDC), a plastic scintillator time-of-flight (TOF) system, and a CsI(Tl) electromagnetic calorimeter (EMC), which are all enclosed in a superconducting solenoid magnet with a field strength of 1.0 T (0.9 T in 2012). The solenoid is supported by an octagonal flux-return yoke with resistive plate counter modules interleaved with steel as a muon identifier. The acceptance for charged particles and photons is 93% over the 4π stereo angle. The charged-particle momentum resolution at 1 GeV/c is 0.5%, and the photon energy resolution at 1 GeV is 2.5% (5%) in the barrel (end-caps) of the EMC. The time resolution in the TOF barrel region is 68 ps, while that in the end cap region was 110 ps. The end cap TOF system was upgraded in 2015 using multi-gap resistive plate chamber technology, providing a time resolution of 60 ps. The MDC encountered the Malter effect due to cathode aging during $\psi(3686)$ data taking in 2012. This effect was suppressed by mixing about 0.2% water vapor into the MDC operating gas [6] and can be well modeled by Monte Carlo (MC) simulation. The other sub-detectors worked well during 2009, 2012, and 2021 operation.

The BESIII detector is modeled with a MC simulation based on GEANT4 [7]. The $\psi(3686)$ produced in the electron-positron collisions are simulated with

the generator KKMC [8], which includes the beam energy spread according to the measurement of BEPCII and the effect of initial state radiation (ISR). The known decay modes of the $\psi(3686)$ are generated with EVTGEN [9] according to the branching fractions from the Particle Data Group [3], while the remaining unknown decays are simulated using the LUNDCHARM model [10]. The MC events are mixed with randomly triggered events (non-physical events from collision) from data to take into account possible effects from beam-related backgrounds, cosmic rays, and electronic noise.

3 Event Selection

The data collected at the $\psi(3686)$ peak includes several different processes, *i.e.*, $\psi(3686) \rightarrow \text{hadrons}$, $\psi(3686) \rightarrow \ell^+\ell^-$ ($\ell = e, \mu$ or τ), ISR return to J/ψ , and nonresonant background including $e^+e^- \rightarrow \gamma^* \rightarrow \text{hadrons}$ ($q\bar{q}$ ($q = u, d, s$)), $e^+e^- \rightarrow \ell^+\ell^-$, and $e^+e^- \rightarrow e^+e^- + X$ ($X = \text{hadrons}, \ell^+\ell^-$). The data also contains non-collision events, *e.g.*, cosmic rays, beam-associated backgrounds, and electronic noise.

To separate the candidate events for $\psi(3686) \rightarrow \text{hadrons}$ from backgrounds, we require that there is at least one charged track candidate in each event. The charged tracks are required to be within 1 cm of the beam line in the plane perpendicular to the beam, within 10 cm from the Interaction Point (IP) in the beam direction and within a polar angle range of $|\cos\theta| < 0.93$, where θ is the angle measured relative to the z axis. Photons reconstructed in the EMC barrel region ($|\cos\theta| < 0.80$) must have a minimum energy of 25 MeV, while those in the end-caps ($0.86 < |\cos\theta| < 0.92$) must have an energy of at least 50 MeV. The photons in the polar angle range between the barrel and end-caps are excluded due to the poor resolution. A requirement of the EMC cluster timing [0, 700] ns is applied to suppress electronic noise and energy deposits unrelated to the event.

The selected hadronic events are classified into three categories according to the multiplicity of good charged tracks (N_{good}), *i.e.*, type-I ($N_{\text{good}}=1$), type-II ($N_{\text{good}}=2$) and type-III ($N_{\text{good}} > 2$). For the type-III events, no further selection criteria are required.

For the type-II events, the momenta of the two charged tracks (p_1 and p_2) are required to be less than 1.7 GeV/c and the opening angle between them (Δ_α) is required to be less than 176° to suppress Bhabha ($e^+e^- \rightarrow e^+e^-$) and dimuon ($e^+e^- \rightarrow \mu^+\mu^-$) backgrounds. Figure 1 shows the distributions of p_2 versus p_1 and Δ_α for the type-II events from the

simulated Bhabha and inclusive $\psi(3686)$ MC samples. Furthermore, a requirement of $E_{\text{visible}}/E_{\text{cm}} > 0.4$ is applied to suppress the low energy background (LEB), which may comprise $e^+e^- \rightarrow e^+e^- + X$, double ISR events ($e^+e^- \rightarrow \gamma_{\text{ISR}}\gamma_{\text{ISR}}X$), *etc.* Here, E_{visible} is the visible energy which is the sum of the energy of all the charged tracks calculated with the track momentum assuming the tracks to be pions and all the neutral showers. Figure 2(left) shows the $E_{\text{visible}}/E_{\text{cm}}$ distributions of the type-II events for the $\psi(3686)$ data and inclusive MC samples. The visible excess in inclusive MC at low energy is from $\psi(3686) \rightarrow \pi^+\pi^- J/\psi$, $J/\psi \rightarrow e^+e^-$, $\mu^+\mu^-$ where the lepton pair is missing. Unless noted, in all plots, the points with error bars are the $\psi(3686)$ data sample collected in 2021, and the histogram is the corresponding inclusive MC sample.

For the type-I events, at least two photons are required in the event. Compared to those events with high charged track multiplicity, the type-I sample has more background according to the vertex distribution of the charged tracks. Thus, a neutral hadron π^0 candidate is required to improve the suppression of background events [4], where the π^0 candidate is reconstructed from a $\gamma\gamma$ pair. Within each event, only the $\gamma\gamma$ candidate with invariant mass closest to the π^0 nominal mass and satisfying $|M_{\gamma\gamma} - M_{\pi^0}| < 0.015$ GeV/ c^2 is kept for further analysis. Figure 3 shows the $M_{\gamma\gamma}$ distribution of the selected π^0 candidates for type-I events. With the above selection criteria, the corresponding $E_{\text{visible}}/E_{\text{cm}}$ distributions of the candidate events for the $\psi(3686)$ data and inclusive MC samples are shown in Fig. 2(right). An additional requirement of $E_{\text{visible}}/E_{\text{cm}} > 0.4$ is also used to suppress the LEB events.

Type-II and type-III events are required to pass a vertex fit that constrains all charged tracks to come from a common vertex. The signal yield of $e^+e^- \rightarrow \text{hadrons}$ is obtained by examining the event vertex distribution, V_Z , defined as the average V_z weighted over all charged tracks in each event. Figure 4 shows the distributions of V_Z for $\psi(3686)$ and off-resonance data samples. The region $|V_Z| < 4$ cm is regarded as the signal region, and the region $6 < |V_Z| < 10$ cm is taken as the sideband region. Events in the sideband region are mainly from non-collision background events. The number of observed hadronic events (N^{obs}) is determined by

$$N^{\text{obs}} = N_{\text{signal}} - N_{\text{sideband}}, \quad (1)$$

where N_{signal} and N_{sideband} are the numbers of events in the signal and sideband regions, respectively.

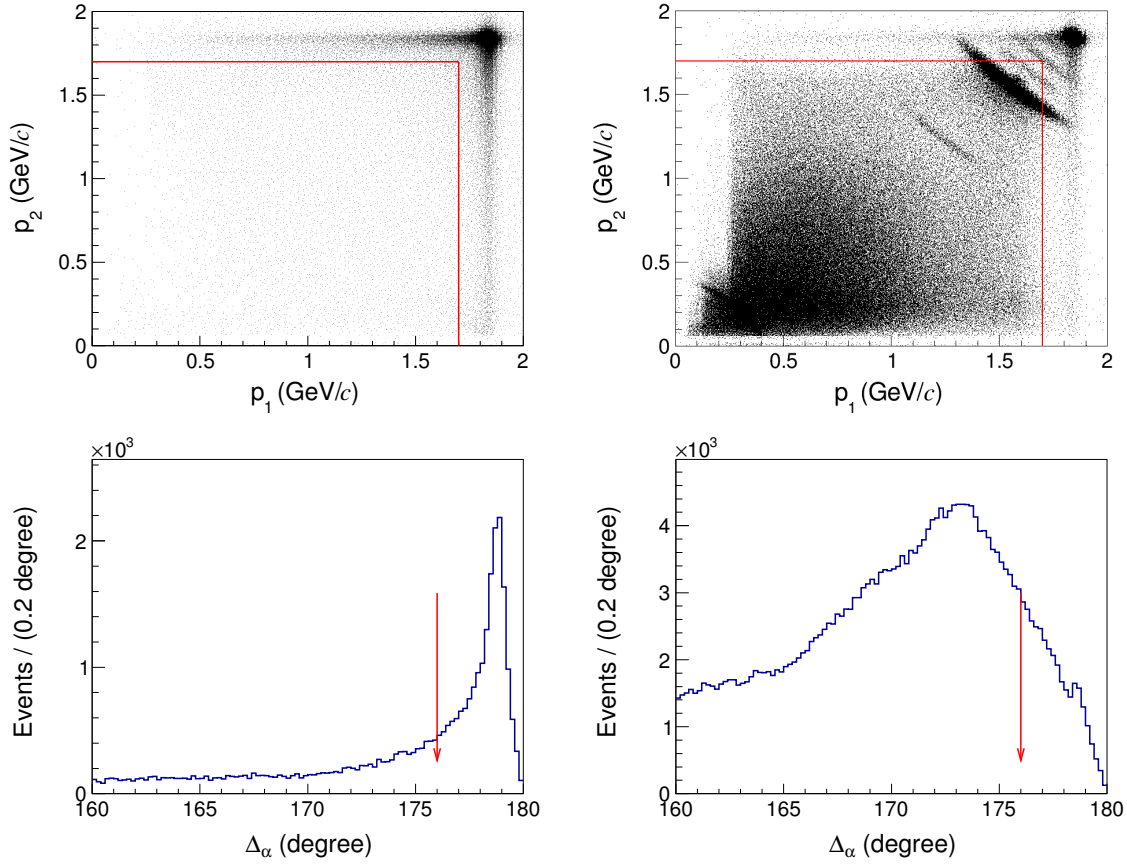


Figure 1: Distributions of p_2 versus p_1 (top) and Δ_α (bottom) for the type-II events from the (left) simulated Bhabha and (right) $\psi(3686)$ inclusive MC samples. The events satisfying $p < 1.7$ GeV/c and $\Delta_\alpha < 176^\circ$ are kept for further analysis. In the top-right plot, the event accumulation in the top-right corner comes from $\psi(3686) \rightarrow e^+e^-, \mu^+\mu^-$, while the different event bands come from $\psi(3686) \rightarrow \text{neutral} + J/\psi$, $J/\psi \rightarrow e^+e^-, \mu^+\mu^-$, etc., and the event band in the bottom-left comes from $\psi(3686) \rightarrow \pi^+\pi^- J/\psi$, $J/\psi \rightarrow e^+e^-, \mu^+\mu^-$ where the lepton pair is missing.

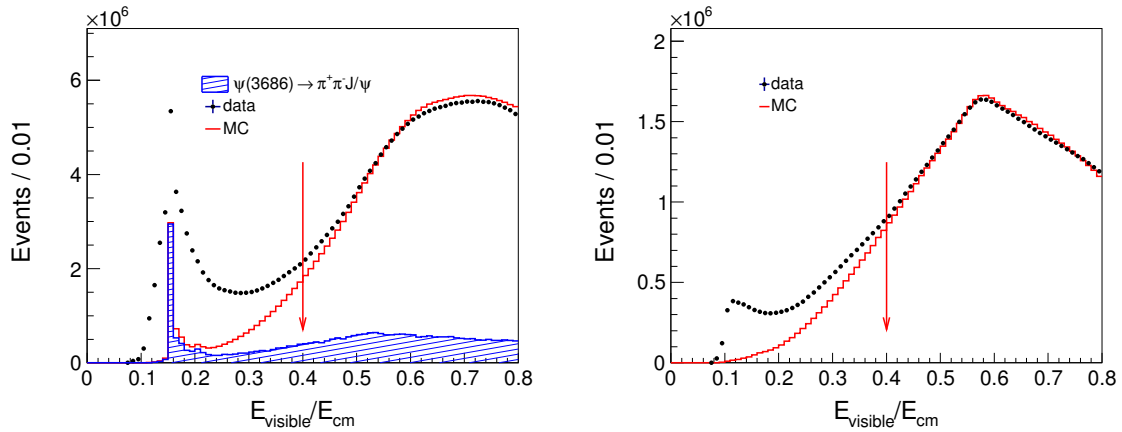


Figure 2: Distributions of $E_{\text{visible}}/E_{\text{cm}}$ for the type-II (left) and type-I (right) events of the $\psi(3686)$ data and inclusive MC samples. The MC distributions have been scaled to data by using events with $E_{\text{visible}}/E_{\text{cm}} > 0.4$. The events lying above the red arrows are kept for further analysis.

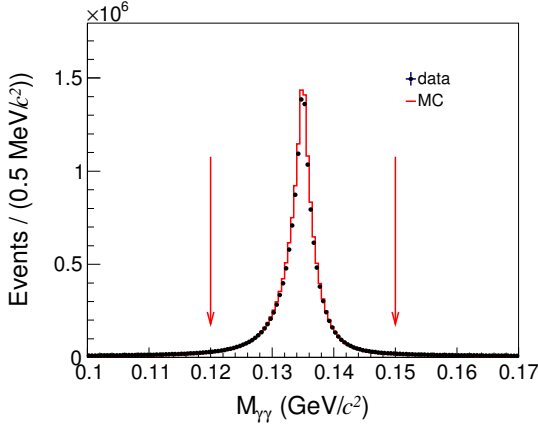


Figure 3: Distribution of $M_{\gamma\gamma}$ for the π^0 candidates from the type-I events. The region within the pair of red arrows is the π^0 signal window.

4 Background Analysis

Following our previous measurement [4], the number of remaining $q\bar{q}$ background events is estimated using the off-resonance data sample due to the small difference in the c.m. energies. We apply the same approach to determine the yields of collision events for the off-resonance data samples, then estimate the contribution at the $\psi(3686)$ resonance after scaling by integrated luminosity. Similarly, the backgrounds from the ISR return to J/ψ are estimated by the same method. The connection between two energy points can be expressed by a scaling factor, f , determined from the integrated luminosity multiplied by $1/s$ to account for the energy dependence of the cross section. This can be done since the dominant backgrounds comes from the Bhabha and dimuon processes at the leading-order contribution [11]. The scale factor is

$$f = \frac{\mathcal{L}_{\psi(3686)}}{\mathcal{L}_{\text{off-res}}} \cdot \frac{3.65^2}{3.686^2}, \quad (2)$$

where $\mathcal{L}_{\psi(3686)}$ and $\mathcal{L}_{\text{off-res}}$ are the integrated luminosities of the $\psi(3686)$ data and off-resonance data samples, and 3.686^2 and 3.65^2 are the corresponding squares of c.m. energies, respectively.

The integrated luminosities at different energy points are determined using Bhabha events [12] with the following selection criteria. The number of charged tracks is required to be equal to two with net charge zero. Each track must have energy deposited in the EMC between 1.0 GeV and 2.5 GeV and a momentum less than $0.5 \times E_{\text{cm}} + 0.3$ GeV. Furthermore, the sum of the momenta of the positron and electron must be greater than $0.9 \times E_{\text{cm}}$. The cosine of

the polar angle (θ) for each track is required to be within $|\cos\theta| < 0.8$ and their ϕ angles must satisfy $5^\circ < ||\phi_1 - \phi_2| - 180^\circ| < 40^\circ$. The luminosities of the $\psi(3686)$ and off-resonance data samples taken in 2021 are 3208.5 pb^{-1} and 401.0 pb^{-1} , with uncertainties of about 1%, respectively.

To test if the interference between Bhabha events and $\psi(3686) \rightarrow e^+e^-$ events affects the luminosity measurement, we examine the integrated luminosities of the $\psi(3686)$ data samples using $e^+e^- \rightarrow \gamma\gamma$ events with the following selection criteria. The number of showers is required to be greater than or equal to two with no candidate charged tracks. Each shower must have deposited energy in the EMC between 1.0 GeV and 2.5 GeV. The cosine of the polar angle (θ) for each shower is required to be within $|\cos\theta| < 0.8$. The two most energetic showers are required to be back to back ($||\theta_1 - 90^\circ| - |\theta_2 - 90^\circ|| < 10^\circ$) and with ϕ angles $||\phi_1 - \phi_2| - 180^\circ| < 2^\circ$. The difference of the measured luminosities is less than 0.1%.

The integrated luminosities of the two off-resonance data samples collected at $E_{\text{cm}} = 3.65$ GeV in 2009 and 2021 are 44.5 and 401.0 pb^{-1} , respectively. The former one is used to estimate the continuum contribution of the 2009 $\psi(3686)$ data sample, and the latter one is used to estimate the continuum contribution of the 2012 and 2021 $\psi(3686)$ data samples. The integrated luminosities of the 2009, 2012, and 2021 $\psi(3686)$ data samples are 161.6 , 506.9 , and 3208.5 pb^{-1} , respectively, with scaling factors f of 3.56 , 1.24 , and 7.85 , respectively. The systematic uncertainties of the luminosities for the two c.m. energies almost cancel when calculating the scaling factors due to the small energy difference.

The cross sections for $e^+e^- \rightarrow \tau^+\tau^-$ are calculated to be 1.84 and 2.14 nb at $E_{\text{cm}} = 3.65$ GeV and 3.686 GeV, respectively. Since the above energy points are close to the $\tau^+\tau^-$ mass threshold, the production cross section does not follow a $1/s$ distribution. Thus, only part of the $e^+e^- \rightarrow \tau^+\tau^-$ background events is included in the off-resonance data samples. To subtract the full background from $e^+e^- \rightarrow \tau^+\tau^-$, we estimate the remaining contribution, $N_{\tau^+\tau^-}^{\text{uncanceled}}$, using the detection efficiency from the MC simulation, the cross section difference at the two c.m. energy points, and the luminosity at the $\psi(3686)$ peak. The estimated residual $e^+e^- \rightarrow \tau^+\tau^-$ background yields are shown in Table 1.

The cross section from the ISR return to J/ψ is also found to slightly violate the $1/s$ distribution. However, the corrected cross section difference for this process at the $\psi(3686)$ peak is about 0.1 nb , which

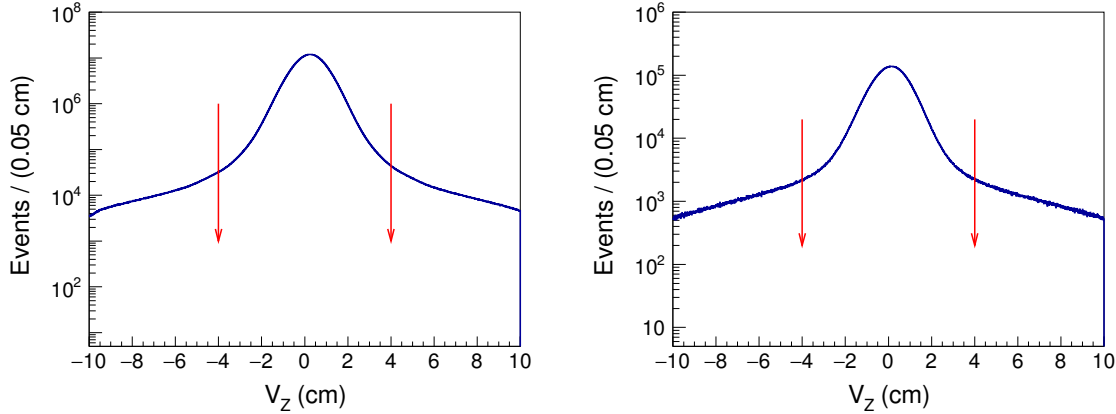


Figure 4: The distributions of V_Z for the accepted hadronic events of the (left) $\psi(3686)$ data and (right) off-resonance data. The region within the pair of red arrows is the signal region.

is negligible if compared to the total observed cross section of $\psi(3686) \rightarrow \text{hadrons}$, ~ 700 nb.

A small fraction of $\psi(3686) \rightarrow \ell^+\ell^-$ events survives the event selection. Since their effect has been considered in the detection efficiency, no further subtraction is made.

Figure 5 shows the comparisons of the distributions of $\cos\theta$, $E_{\text{visible}}/E_{\text{cm}}$, N_{good} , and photon multiplicity (N_γ) after background subtraction between data and MC simulation, and a reasonable data-MC agreement is observed. Table 1 summarizes the numbers of the observed hadronic events for different N_{good} requirements of $\psi(3686)$ data ($N_{\psi(3686)}^{\text{obs}}$) and off-resonance data ($N_{\text{off-res}}^{\text{obs}}$). The detection efficiencies of $\psi(3686) \rightarrow \text{hadrons}$ are determined with 2.3 billion $\psi(3686)$ inclusive MC events, where the branching fraction of $\psi(3686) \rightarrow \text{hadrons}$ is included in the efficiency.

5 Numerical Results

With the numbers listed in Table 1, we determine the number of $\psi(3686)$ events using

$$N_{\psi(3686)} = \frac{N_{\psi(3686)}^{\text{obs}} - f \cdot N_{\text{off-res}}^{\text{obs}} - N_{\tau^+\tau^-}^{\text{uncanceled}}}{\epsilon}. \quad (3)$$

The obtained numerical results for $N_{\psi(3686)}$ with different N_{good} requirements are slightly different with each other, mainly due to the imperfect simulation of the charged track multiplicity. To obtain a more accurate $N_{\psi(3686)}$, an unfolding method is employed based on an efficiency matrix determined from the $\psi(3686)$ inclusive MC sample. In practice, there are even numbers of charged tracks generated in an event due to charge conservation, while any number of charged tracks can be observed due to the reconstruction ef-

ficiency and backgrounds. Therefore, the true multiplicities of charged tracks of the data sample is estimated from the observed multiplicities of charged tracks and the efficiency matrix by minimizing the χ^2 , defined as

$$\chi^2 = \sum_{i=0}^{10} \frac{(N_i^{\text{obs}} - \sum_{j=0}^{10} \epsilon_{ij} \cdot N_j)^2}{N_i^{\text{obs}}}, \quad (4)$$

where the values N_i^{obs} ($i = 0, 1, 2, \dots$) are the observed multiplicities of charged tracks in the data sample corresponding to the distribution in Fig. 5 (bottom-left, the points with error bars), the matrix elements ϵ_{ij} represent the probability to observe i charged tracks for an event with j actual charged tracks, and the values N_j ($j = 0, 2, 4, \dots$) are the true multiplicities of charged tracks in the data sample. They are free parameters in the fit. For simplicity, the events with ten or more charged tracks are combined in the number N_{10} . The $N_{\psi(3686)}$ is calculated by summing over all the obtained N_j . The results are 107.7×10^6 , 345.4×10^6 and 2259.3×10^6 for the 2009, 2012 and 2021 data samples, respectively.

6 Systematic Uncertainties

The systematic uncertainties in the $N_{\psi(3686)}$ measurement from different sources are described below and listed in Table 2.

6.1 Polar angle of charged tracks

The polar angles of charged tracks are required to satisfy $|\cos\theta| < 0.93$. To estimate the relevant systematic uncertainty, we redo the measurement with an alternative requirement of $|\cos\theta| < 0.8$. The difference in the measured number of $\psi(3686)$ events is taken as the systematic uncertainty.

Table 1: Number of hadronic events $N_{\psi(3686)}^{\text{obs}}$ in the $\psi(3686)$ data, separately for different requirements on the number of good tracks N_{good} , where $N_{\psi(3686)}^{\text{obs}}$ is the number of hadronic events observed in the $\psi(3686)$ data, f is the scaling factor, $N_{\text{off-res}}^{\text{obs}}$ is the number of hadronic events observed in the off-resonance data, $N_{\tau^+\tau^-}^{\text{uncanceled}}$ is the number of remaining $e^+e^- \rightarrow \tau^+\tau^-$ events after subtracting the normalized off-resonance data, ϵ is the detection efficiency, and $N_{\psi(3686)}$ is the determined number of $\psi(3686)$ events.

Multiplicity	$N_{\text{good}} \geq 1$			$N_{\text{good}} \geq 2$			$N_{\text{good}} \geq 3$		
Year	2009	2012	2021	2009	2012	2021	2009	2012	2021
$N_{\psi(3686)}^{\text{obs}} (10^6)$	107.98	345.14	2246.93	104.77	333.79	2172.16	83.36	264.57	1722.56
f	3.56	1.24	7.85	3.56	1.24	7.85	3.56	1.24	7.85
$N_{\text{off-res}}^{\text{obs}} (10^6)$	2.05	18.18	18.18	1.99	17.65	17.65	0.75	6.51	6.51
$N_{\tau^+\tau^-}^{\text{uncanceled}} (10^6)$	0.04	0.13	0.80	0.04	0.12	0.76	0.01	0.03	0.22
ϵ (%)	93.21	92.83	92.86	90.42	89.65	89.86	74.69	73.39	73.85
$N_{\psi(3686)} (10^6)$	107.96	347.36	2265.08	107.99	347.75	2262.32	108.03	349.46	2262.94

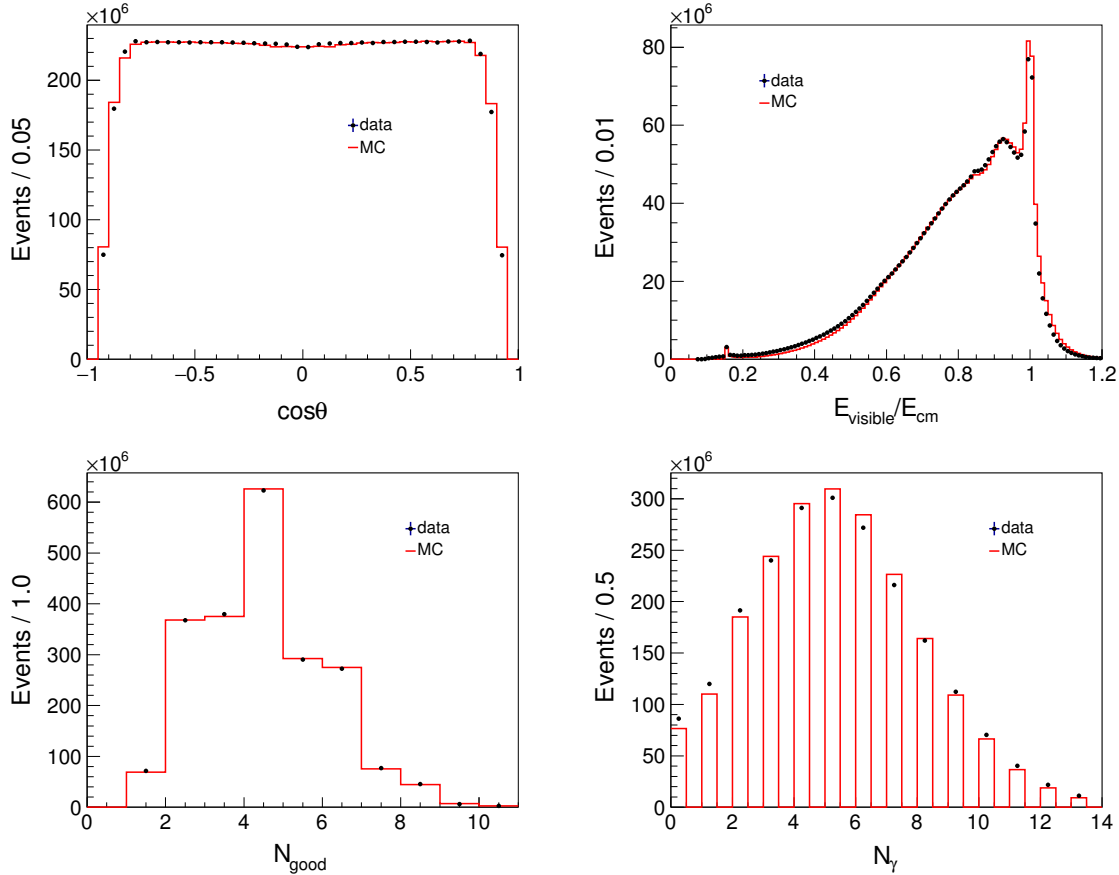


Figure 5: Comparisons of the distributions of (top-left) $\cos\theta$, (top-right) $E_{\text{visible}}/E_{\text{cm}}$, (bottom-left) N_{good} , and (bottom-right) N_{γ} between $\psi(3686)$ data and inclusive MC samples after background subtraction.

6.2 Tracking efficiency

The systematic uncertainties due to the tracking efficiency for both the 2009 and 2012 data samples have been found to be negligible based on various studies [4]. Therefore, the associated systematic uncertainty for the 2021 data sample is also ignored.

6.3 Charged track multiplicity

To estimate the systematic uncertainty arising from the charged track multiplicity, we compare the directly calculated result as shown in Table 1 and that obtained with the unfolding method after including the $N_{\text{good}} \leq 1$ events. The differences in the number of $\psi(3686)$ events for the 2009, 2012 and 2021 data samples, which are 0.24%, 0.56%, and 0.26%, respectively, are taken as individual systematic uncertainties.

6.4 Momentum and opening angle

To estimate the systematic uncertainty due to the requirement on charged track momentum for the type-II events, we vary the nominal requirement from $p < 1.7 \text{ GeV}/c$ to $p < 1.55 \text{ GeV}/c$, and the opening angle between two charged tracks from $\theta < 176^\circ$ to $\theta < 160^\circ$. The change in $N_{\psi(3686)}$ is taken as the corresponding systematic uncertainty.

6.5 LEB contamination

In the nominal measurement, the $E_{\text{visible}}/E_{\text{cm}} < 0.4$ requirement is used to suppress the LEB background events for the type-I and type-II events. The systematic uncertainty due to this requirement is assigned with alternative requirements of $E_{\text{visible}}/E_{\text{cm}} < 0.35$ and $E_{\text{visible}}/E_{\text{cm}} < 0.45$. The larger change in $N_{\psi(3686)}$ is assigned as the systematic uncertainty.

6.6 Extraction method of N^{obs}

The nominal measurement is performed by counting the events in the V_z distributions in Fig. 4. To examine the systematic uncertainty associated with the counting method, we use an alternative method by fitting the V_z distributions with three linearly added Gaussian functions to model the signal shape and a second order polynomial function to describe the non-collision background. The difference in the determined $N_{\psi(3686)}$ values between these two methods is taken as the systematic uncertainty.

6.7 Vertex requirement

To estimate the systematic uncertainties due to the vertex requirement, we examine the number of

$\psi(3686)$ events after varying the nominal vertex requirements of $V_r < 1 \text{ cm}$ to $V_r < 2 \text{ cm}$, and from $|V_z| < 10 \text{ cm}$ to $|V_z| < 15 \text{ cm}$. The change in the measured number of $\psi(3686)$ events is taken as the systematic uncertainty.

6.8 Scaling factor

The systematic uncertainty due to the scaling factor f is estimated with the alternatively measured luminosities with $e^+e^- \rightarrow \gamma\gamma$ events. The change of the re-measured $N_{\psi(3686)}$ is found to be negligible and this systematic uncertainty is therefore neglected.

6.9 π^0 mass requirement

A requirement of $|M_{\gamma\gamma} - M_{\pi^0}| < 0.015 \text{ GeV}/c^2$ has been imposed on the type-I events to suppress background. Its effect on the measured number of $\psi(3686)$ events is studied with an alternative requirement of $|M_{\gamma\gamma} - M_{\pi^0}| < 0.025 \text{ GeV}/c^2$. The change in $N_{\psi(3686)}$ is taken as the systematic uncertainty.

6.10 Missing $N_{\text{good}} = 0$ hadronic events

We do not consider the $N_{\text{good}} = 0$ hadronic events in the nominal measurement. The topological analysis for the $\psi(3686)$ inclusive MC samples shows that most of these events come from well-known decay channels, such as $\psi(3686) \rightarrow X + J/\psi$ (where X denotes η , π^0 , $\pi^0\pi^0$, $\gamma\gamma$, etc.) and $\psi(3686) \rightarrow e^+e^-$, $\mu^+\mu^-$. The fraction of $N_{\text{good}} = 0$ hadronic events is $\sim 2.0\%$, and the pure neutral channels contribute about 1.0% .

We examine the effect of the $N_{\text{good}} = 0$ hadronic events as follows. A sample is selected using the requirements $N_{\text{good}} = 0$ and $N_\gamma > 3$, where the good charged tracks and showers are selected with the same criteria mentioned above. The $N_\gamma > 3$ requirement is used to suppress the $e^+e^- \rightarrow \gamma\gamma$ and beam-associated background events. Figure 6 shows the distributions of the total energy in the EMC, E_{EMC} , for the different data sets and inclusive MC samples. The events concentrated around the c.m. energy are mainly from the pure neutral hadronic candidates. The number of signal events is determined by a fit to the E_{EMC} distribution. In this fit, the signal is described by a Crystal Ball function, the nonresonant background in the $\psi(3686)$ data sample is described by the shape of off-resonance data sample after luminosity normalization, and the other backgrounds are described by a polynomial function. For the 2021 data sample, the difference in the number of pure neutral hadronic events between the $\psi(3686)$ data and inclusive MC samples is 11%. Since the fraction of the pure neu-

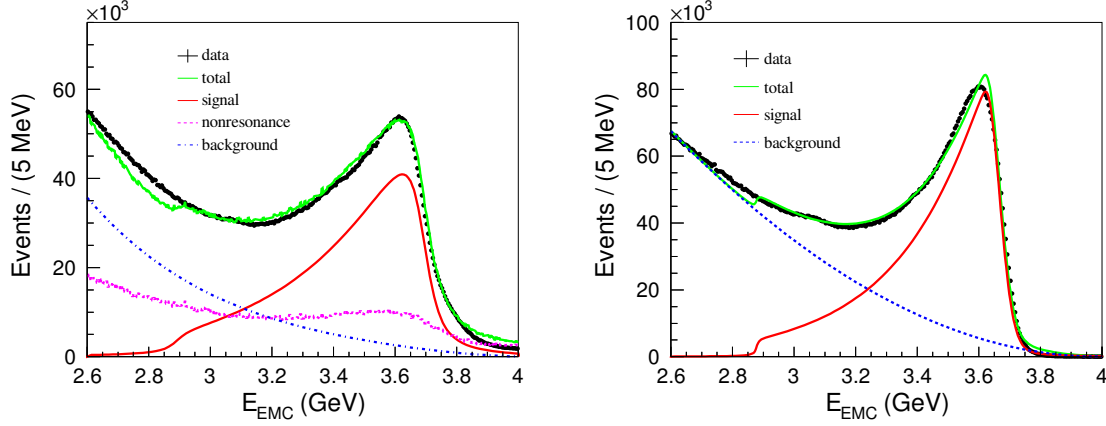


Figure 6: Distributions of E_{EMC} for the $N_{\text{good}} = 0$ hadronic events from the $\psi(3686)$ data (left) and inclusive MC (right) samples. The black points with error bar are data. The red lines are the signal shapes of neutral $\psi(3686)$ decays, the blue lines are the background shapes from $\psi(3686)$ decays, the pink line is the total background shape from nonresonant processes, and the green lines are the final fit curves.

Table 2: Relative systematic uncertainties (%) in the determination of the number of $\psi(3686)$ events.

Source	2009	2012	2021
Polar angle of charged track	0.25	0.20	0.22
Tracking efficiency	negligible	negligible	negligible
Charged track multiplicity	0.24	0.56	0.26
Momentum and opening angle	0.20	0.26	0.26
LEB contamination	0.02	0.04	0.12
Extraction method of N^{obs}	0.16	0.16	0.03
Vertex requirement	0.13	0.08	0.07
Scaling factor (f)	negligible	negligible	negligible
π^0 mass requirement	negligible	0.01	0.05
Missing $N_{\text{good}} = 0$ hadronic events	0.38	0.31	0.11
MC modeling	negligible	negligible	negligible
Trigger efficiency	negligible	negligible	negligible
$\mathcal{B}(\psi(3686) \rightarrow \text{hadrons})$	0.13	0.13	0.13
Total	0.60	0.75	0.49

tral hadronic events is about 1% of the total selected hadronic events, the systematic uncertainty due to the missing $N_{\text{good}} = 0$ hadronic events must be less than $11\% \times 1\% = 0.11\%$ for the 2021 data sample. With the same method, the systematic uncertainties for the 2009 and 2012 data samples are assigned as 0.38% and 0.31%, respectively.

6.11 MC modeling

The systematic uncertainties due to MC modeling include the input branching fractions and the angular distributions of the known and unknown decay modes in the $\psi(3686)$ inclusive MC sample. These uncertainties have been covered by those of the charged track multiplicity and the missing $N_{\text{good}} = 0$ events. Hence no systematic uncertainty is assigned for the MC modeling.

6.12 Trigger efficiency

The trigger efficiencies for BESIII data were studied in 2010 [13] and 2021 [14]. The trigger efficiency for the $N_{\text{good}} \geq 2$ (type-II and type-III) events is found to be close to 100.0%, while it is 98.7% for the type-I events [13]. Since the fraction of the type-I events is only about 3% of the total selected hadronic events, the associated systematic uncertainty is negligible. The neutral channel trigger has been added since 2012, and the trigger efficiency for the type-I events is expected to be higher than before. Therefore, the systematic uncertainty associated with the trigger efficiency is negligible.

6.13 Branching fraction of $\psi(3686) \rightarrow \text{hadrons}$

The uncertainty of the branching fraction of $\psi(3686) \rightarrow \text{hadrons}$, 0.13% [1–3], is taken as a systematic uncertainty.

6.14 Total systematic uncertainty

The total systematic uncertainty for each $\psi(3686)$ data sample is obtained as the quadratic sum of all the systematic uncertainties.

7 Summary

By analyzing inclusive hadronic events, the number of $\psi(3686)$ events taken by the BESIII detector in 2021 is measured to be $(2259.3 \pm 11.1) \times 10^6$, where the uncertainty is systematic and the statistical uncertainty is negligible. The numbers of $\psi(3686)$ events taken in 2009 and 2012 are also updated to be $(107.7 \pm 0.6) \times 10^6$ and $(345.4 \pm 2.6) \times 10^6$, respectively. Both are consistent with the previous measurements within one standard deviation, and a slight difference in the 2012 $\psi(3686)$ events relative to the previous one is caused by changing the off-resonance data from the previous τ -scan data to the off-resonance data at $\sqrt{s} = 3.65$ GeV in 2021. The total number of $\psi(3686)$ events for the three data samples is obtained to be $(2712.4 \pm 14.3) \times 10^6$ by adding the above three yields linearly. This work provides an important parameter used in precision measurements of decays of the $\psi(3686)$ and its daughter charmonium particles.

The BESIII collaboration thanks the staff of BEPCII and the IHEP computing center for their strong support.

References

- 1 V. Luth, A. Boyarski, H. L. Lynch, M. Breidenbach, F. Bulos, G. J. Feldman, D. Fryberger, G. Hanson, R. R. Larsen and D. Luke, *et al.* Phys. Rev. Lett. **35**, 1124-1126 (1975).
- 2 J. Z. Bai *et al.* (BES Collaboration), Phys. Lett. B **550**, 24-32 (2002).
- 3 R. L. Workman *et al.* (Particle Data Group), PTEP **2022**, 083C01 (2022).
- 4 M. Ablikim *et al.* (BESIII Collaboration), Chin. Phys. C **42**, 023001 (2018).
- 5 M. Ablikim *et al.* (BESIII Collaboration), Nucl. Instrum. Meth. A **614**, 345-399 (2010).
- 6 M. Y. Dong, Q. L. Xiu, L. H. Wu, Z. Wu, Z. H. Qin, P. Shen, F. F. An, X. D. Ju, Y. Liu and K. Zhu, *et al.* Chin. Phys. C **40**, 016001 (2016).
- 7 J. Allison, K. Amako, J. Apostolakis, H. Araujo, P. A. Dubois, M. Asai, G. Barrand, R. Capra, S. Chauvie and R. Chytrcek, *et al.* IEEE Trans. Nucl. Sci. **53**, 270 (2006).
- 8 S. Jadach, B. F. L. Ward and Z. Was, Phys. Rev. D **63**, 113009 (2001).
- 9 R. G. Ping, Chin. Phys. C **32**, 599 (2008).
- 10 J. C. Chen, G. S. Huang, X. R. Qi, D. H. Zhang and Y. S. Zhu, Phys. Rev. D **62**, 034003 (2000).
- 11 G. Balossini, C. M. Carloni Calame, G. Montagna, O. Nicrosini and F. Piccinini, Nucl. Phys. B **758**, 227-253 (2006).
- 12 M. Ablikim *et al.* (BESIII Collaboration), Chin. Phys. C **37**, 123001 (2013).
- 13 N. Berger, K. Zhu, Z. A. Liu, D. P. Jin, H. Xu, W. X. Gong, K. Wang and G. F. Cao, Chin. Phys. C **34**, 1779-1784 (2010).
- 14 M. Ablikim *et al.* (BESIII Collaboration), Chin. Phys. C **45**, 023002 (2021).